Proceedings of the Fifth International Conference on Nanochannels, Microchannels and Minichannels
ICNMM2007
June 18-20, 2007, Puebla, Mexico

ICNMM2007-30141

EFFECT OF INLET GEOMETRY ON ADIABATIC GAS-LIQUID TWO-PHASE FLOW IN A MICROCHANNEL

Hideo Ide
Dept. of Mechanical Engineering
Kagoshima University
Kagoshima, Japan

Ryuji Kimura
Dept. of Mechanical Engineering
Kagoshima University
Kagoshima, Japan

Masahiro Kawaji
Dept. of Chemical Engineering
and Applied Chemistry,
University of Toronto
Canada

ABSTRACT

An optical measurement system and video camera were used to investigate gas-liquid two-phase flow characteristics in a circular microchannel of 100 μm diameter. By cross correlating the signals from two pairs of optical fibers and infrared photodiodes, void fraction and the lengths and velocities of gas slugs and liquid slugs were measured. The data were obtained using a T-junction with the same internal diameter as the microchannel but the lengths of the gas and liquid injection lines between the T-junction and flow control valves were quite different. The presence of a large compressible gas volume upstream of the T-junction had a significant effect on the two-phase flow characteristics in the microchannel, typified by the void fraction data. The two-phase flow characteristics in the absence of a compressible gas volume were analysed to obtain the liquid slug length and velocity data. The liquid slug velocity was found to be dependent on the slug length, since longer slugs experienced greater friction effects and moved with much slower velocities than the shorter liquid slugs.

INTRODUCTION

Ide et al. (2006) developed an optical system to detect the passage of gas plugs and liquid slugs in a 100 μm diameter microchannel. The system consisted of five sets of an LED (wavelength = 644 nm), an optical fiber with a core diameter of 250 μm, and a photodetector. A total of four fibers were placed 0.25 mm apart and the light transmitted across the transparent microchannel was guided through 250 μm core optical fibers to the photodetectors. All the optical fibers and the microchannel were embedded in the plastic plate to align the axes of each pair of optical fibers.

By cross correlating the signals from two pairs of optical fibers and infrared photodiodes, void fraction and the lengths and velocities of gas slugs and liquid slugs were measured. The data were obtained using nitrogen gas and water as the working fluids, which were mixed in a 100 μm diameter T-junction upstream of the microchannel inlet as shown in Fig. 1. The flow control valves were placed upstream of 2.0-m long, 250 μm inner diameter tubes.

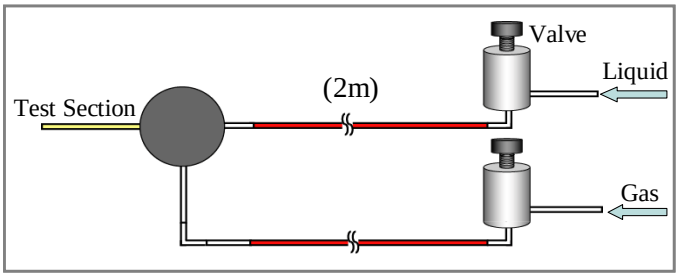

Fig. 1 Liquid and gas mixing in a T-junction (Case 1)

The void fraction data obtained with the gas-liquid mixing method and inlet geometry as shown in Fig. 1 agreed with the following correlation developed by Kawahara et al. (2002) for microchannels.

$$\alpha = \frac{C_1 \beta^{0.5}}{1 - C_2 \beta^{0.5}} \qquad (1)$$

Here, α is the void fraction, $\beta = j_G/(j_G+j_L)$ is the homogeneous void fraction or volumetric quality, and C_1 and C_2 were

constants equal to C_1 = 0.03 and C_2 = 0.97 for the 100 μm circular channel.

Kawahara et al. (2002) obtained Eq. 1 using a gradual contraction inlet where gas and liquid were mixed in a coaxial mixer. Chung and Kawaji (2004) used the same coaxial mixer and a gradually contracting inlet to investigate the two-phase flow of nitrogen gas and water through horizontal circular microchannels of 50 ~ 500 μm diameter. They also obtained a similar void fraction correlation (Eq. 1 with C_1 = 0.02 and C_2 = 0.98) for a 50 μm diameter microchannel.

Recent studies (Kawaji et al., 2005, 2006) have revealed the importance of the inlet geometry and liquid/gas mixing method on the two-phase flow characteristics in a 100 μm microchannel. A reducer inlet and T-junction inlet have been tested and the resulting two-phase flow was classified as pseudo-separated and pseudo-homogeneous two-phase flow, respectively.

In the present work, a T-junction inlet and different gas and liquid inlet lines as described in the next section have been used to determine the effect of the gas inlet volume between the flow control valve and the microchannel.

EXPERIMENTAL APPARATUS AND DATA ANALYSIS

Details of the present experiment are explained below briefly. The reader can refer to Kawahara et al. (2002), Chung and Kawaji (2004) and Ide et al. (2006) for more details not given here. Figure 2 illustrates the basic experimental apparatus used. De-ionized water was driven through a horizontal microchannel by a pneumatic-type pump. Using a 100 μm diameter T-junction, nitrogen gas from a pressurized cylinder was mixed with water upstream of the 100 μm microchannel.

A Valco Nanovolume® 4-way cross connector with an inner bore diameter of 100 μm was used as the T-junction since the fourth line was connected to a pressure transducer to measure the test section inlet pressure. A circular microchannel was made of fused silica with a polyimide coating (Polymicro Technologies) with an inner diameter of 100 μm and an overall length of 71 mm between the gas-liquid mixing point and the exit. The inner surface of the microchannel was silanized by trimethylsilane groups so it became hydrophobic. The window for flow visualization with a video camera was located at 45 mm from the gas-liquid mixing point.

The effect of the overall microchannel length on two-phase flow was also investigated by increasing the overall microchannel length from 71mm in Case 2 to 371 mm in Case 3. In all three Cases, the flow visualization was performed at a location 45 mm, and the optical fiber probes were located at 36 mm downstream of the T-junction.

In the present work, the gas and liquid flow control valves were connected to the T-junction using 250μm inner diameter tubes of 215 mm length for the gas and 135 mm for the liquid injection lines as shown in Fig. 3. A differential pressure transducer (Validyne DP15) was attached to a 2.0-m long, 250μm inner diameter tube upstream of each flow control valve to measure the friction pressure drop and determine the gas or liquid flow rate. This method of flow rate measurement was used to cover low superficial gas velocities in Case 2. The ranges of superficial gas and liquid velocities covered in the present experiments are shown in Table 1.

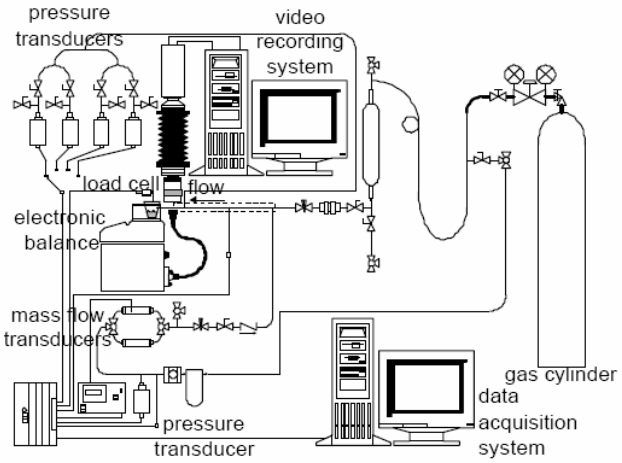

Fig. 2 Experimental apparatus

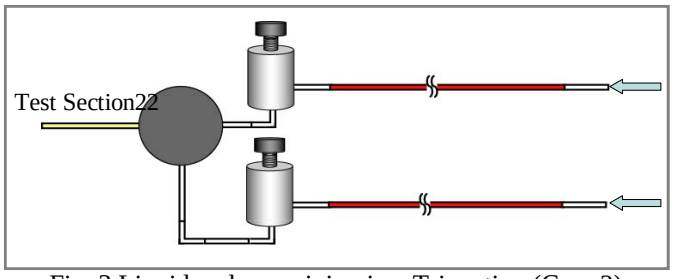

Fig. 3 Liquid and gas mixing in a T-junction (Case 2)

Table 1 Liquid and Gas Flow Rates

	Case 1	Case 2	Case 3
j_L (m/s)	0.1 - 0.4	0.06 - 0.16	0.1 - 0.3
j_G (m/s)	1.5 - 4.0	0.018 - 0.8	0.07 - 0.3

Ide et al. (2006) used the same optical fiber probe system to make local on-line measurements and obtain detailed gas plug and liquid slug length data as well as their velocities. Electrical signals from photodiodes were sampled at over 10 kHz to indicate the presence of gas or liquid phase at the probe location in the microchannel. The data were then analyzed using a threshold signal level to distinguish gas or liquid phase and yield the time average void fraction. Furthermore, by using multiple fiber probes and photodetectors installed along the flow direction at certain intervals, it was possible to measure the speed and length of gas bubbles/plugs and liquid slugs. The time-averaged void fraction data obtained with the optical probe agreed with the ensemble-average void fraction data obtained from video images within ±10%.

In the present paper, the Case 2 results will be mainly presented in the next section.

RESULTS AND DISCUSSION

Flow Patterns

In the Case 2 experiments, the liquid and gas flow rates covered were much lower than in previous Case 1 experiments. The flow patterns observed at these low flow rates were essentially slug flow, but under certain flow conditions, bubbly flow and ring film flow patterns were seen to alternate with the slug flow. Also, some slug flow patterns showed deformed gas slug shapes as shown in Fig. 4.

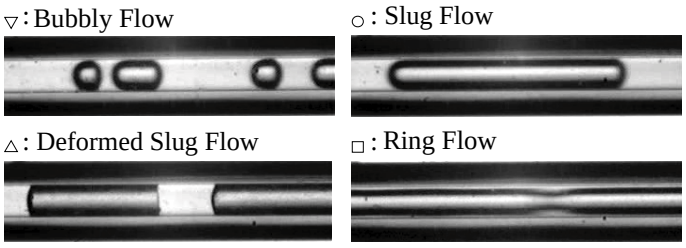

Fig. 4 Typical flow patterns observed in Case 2 experiments

Some gas slugs showed a nearly flat nose and tail as opposed to a semi-spherical shape as shown in Fig. 5 due to the hydrophobicity of the microchannel inner wall. In some cases, under the same gas and liquid flow rates, gas slugs showed semi-spherical nose and tail as well.

The effect of channel wall wettability on static gas bubbles was described by Cabaud et al. (2004). As the wettability of the microchannel wall was changed from hydrophilic (with a contact angle $\theta = 60^{o}$) to hydrophobic ($\theta = 120^{o}$), the nose and tail of the stationary gas plug were shown to change from convex to concave shapes, but the flat nose and tail shapes were not indicated in their paper.

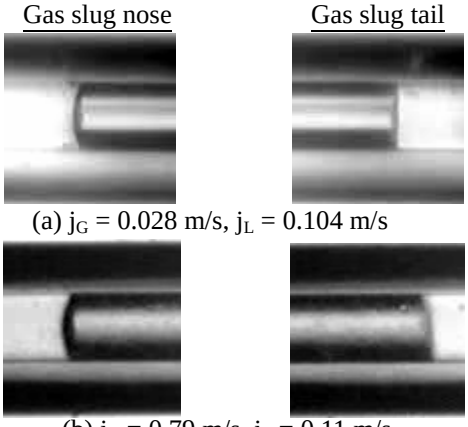

(a) j_G = 0.028 m/s, j_L = 0.104 m/s

(b) j_G = 0.79 m/s, j_L = 0.11 m/s

Fig. 5 Gas slugs with a flat nose and tail

The flow pattern map based on the four flow patterns illustrated in Fig. 4 is shown in Fig. 6. The dotted lines indicate the boundaries between different flow patterns, and dark symbols indicate that some of the gas slugs observed had nearly flat nose and tail. The analysis of the flow pattern data for the Case 3 is underway to determine any effect of the microchannel length on the flow patterns in the near future.

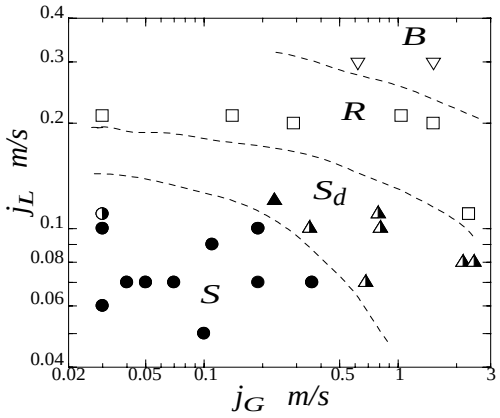

Fig. 6 Two-phase flow pattern map for Case 2 experiments (*B*-bubbly flow; *R*-ring flow; S_d-deformed slug flow; *S*-slug flow)

Time Average Void Fraction

Using a threshold value midway between the maximum and minimum signal levels to distinguish gas and liquid phases in the analysis of optical fiber probe signals, the time fractions of gas and liquid phases were computed from the time series probe data. The time-averaged void fraction data were then obtained and are shown in Figs. 7 and 8.

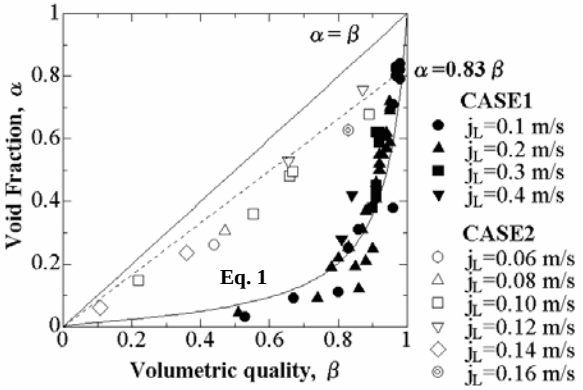

Fig. 7 Void fraction data for Cases 1 and 2

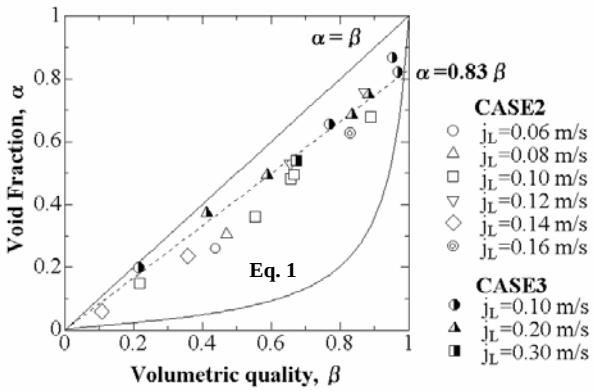

Fig. 8 Void fraction data for Cases 2 and 3

Although a T-junction with the same diameter as the microchannel (D = 100 μm) was used in all three cases, the void fraction data showed large differences between Cases 1 and 2 (Fig. 7). The data for Case 1 shown in Fig. 7 include those presented by Ide et al. (2006) and newly obtained data. The Case 1 data are seen to obey Eq. 1. The presence of a large compressible gas volume upstream of the T-junction inlet in the form of a 2.0-m long, 250 μm tube is thought to cause intermittent gas flow into the T-junction. Although the time-average gas flow rate is unchanged, if the gas injection is intermittent, long gas plugs and liquid slugs are generated downstream of the microchannel. Since the liquid slugs would move slowly due to friction, the residence time of liquid slugs would be large and the time-average void fraction would be reduced.

On the other hand, when the compressible gas volume is eliminated between the flow control valve and the T-junction as in Case 2, the void fraction data obey Armand's (1946) correlation ($\alpha = 0.83\beta$), which is applicable to minichannels with hydraulic diameters between about 1 and 5 mm (Ali et al., 1993). This result adds to our previous findings on the significant effect of inlet geometry and gas-liquid mixing method on the two-phase flow characteristics in a microchannel (Kawaji et al., 2005, 2006).

In the absence of the compressible gas volume upstream of the T-junction, the effect of the microchannel length is seen to be small as similar void fraction data were obtained between Cases 2 and 3 (Fig. 8).

Liquid Plug/Slug Length and Velocity

A sample time history of an optical probe signal for Case 2 at $j_G = 0.19$ m/s and $j_L = 0.10$ m/s is shown in Fig. 9. The relative signal levels, $V/V_o = 0$ and 1, correspond to the gas and liquid phases, respectively. The probe signal clearly indicates alternate passages of liquid and gas plugs/slugs, and occurrence of short liquid plugs and long liquid slugs.

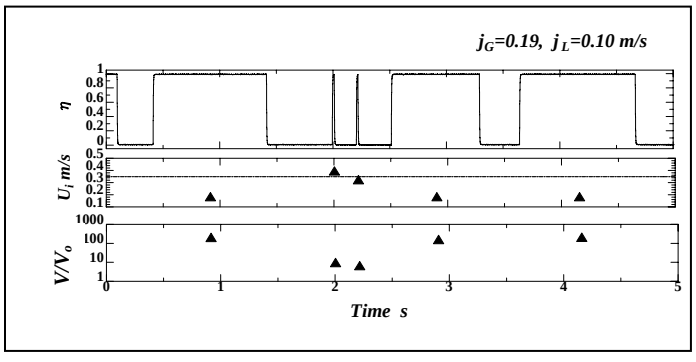

Fig. 9 Optical fiber probe signal and liquid slug velocity and length data

From the cross correlation of two optical probe signals, the velocity of the head of each liquid plug/slug is obtained and shown as *Ui*. The dotted line indicates Hughmark's (1965) equation for the gas slug velocity in horizontal slug flow,

$$u_G = 1.2(j_G + j_L) \qquad (2)$$

By combining the velocity and signal duration, the length of each liquid plug/slug, L_L, could then be computed as shown at the bottom.

In Fig. 9, we can observe that short liquid plugs of about 10 mm length moved at *Ui* = 0.35 m/s, nearly the same velocity as the gas slug velocity given by Eq. 2, while longer liquid slugs of about 100 mm length moved at much slower velocities, *Ui* = 0.2 m/s.

As the superficial gas velocity was increased, the mean liquid plug/slug length decreased as shown in Fig. 10, but it is worthwhile to examine the length distribution of liquid plugs/slugs and their velocities.

The number of liquid slugs detected in 30 seconds is plotted against the liquid slug length in Fig. 11. The frequency of occurrence of short liquid plugs increased while the frequency of the long liquid slugs decreased as the superficial gas velocity, j_G, was increased from 0.07 m/s to 0.81 m/s, at a constant superficial liquid velocity of $j_L = 0.10$ m/s. The mean liquid plug/slug length decreased from 147 mm to 73.8 mm and then to 13.5 mm, and the standard deviation also decreased. The liquid slug frequency vs. length data presented in Fig. 11 and at other gas and liquid flow rates showed both single peak and bimodal distributions.

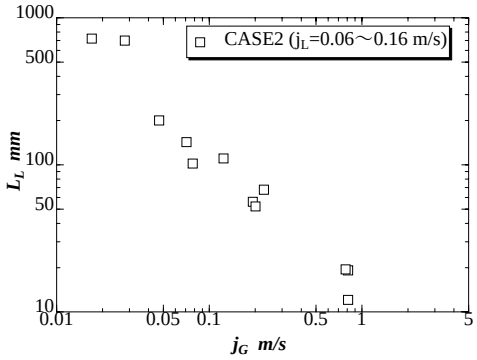

Fig. 10 Variation of mean liquid plug/slug length with superficial gas velocity

The velocities of short liquid plugs, U_H, and long liquid slugs, U_L, are plotted against the sum of the superficial gas and liquid velocities in Fig. 12. The solid line indicates the gas slug velocity given by Eq. 2. The short liquid plugs are seen to move at nearly the same velocity as the gas slugs, while the long liquid slugs moved at much slower velocities. The differences between them increased with an increase in the total superficial velocity.

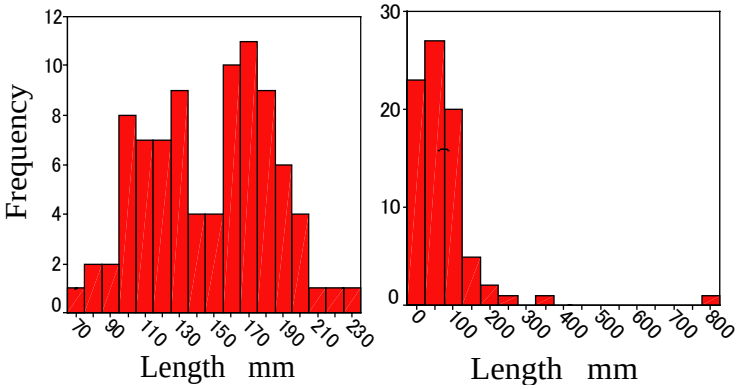

(a) j_G = 0.07 m/s, j_L = 0.10 m/s (b) j_G = 0.19 m/s, j_L = 0.10 m/s

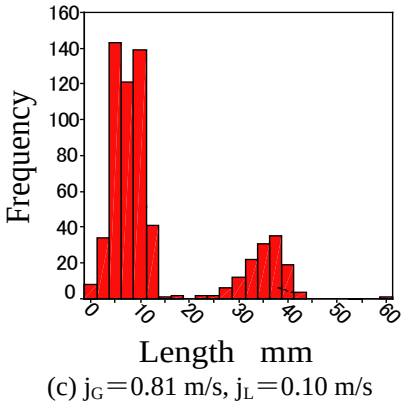

(c) j_G = 0.81 m/s, j_L = 0.10 m/s

Fig. 11 Liquid plug/slug frequency (number per 30 sec) vs. length

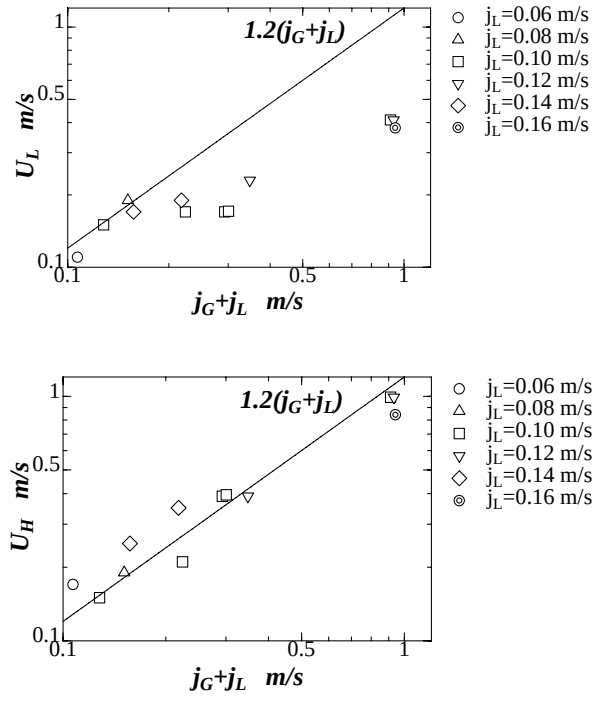

Fig. 12 Velocities of short liquid plugs (U_H) and long slugs (U_L)

CONCLUSION

An optical measurement system was used to investigate the gas-liquid two-phase flow characteristics in a circular microchannel of 100 μm diameter. By using multiple optical fibers and photodiodes, void fraction and liquid plug/slug lengths and their velocities were measured and analyzed for j_L = 0.06 - 0.16 m/s and j_G = 0.018 - 0.8 m/s. Video images showed the two-phase flow patterns in the microchannel to be essentially a slug flow, but depending on the gas and liquid flow rates, bubbly flow, ring flow and deformed slug flow patterns occurred alternating with the slug flow pattern. A two-phase flow pattern map was then developed for the case without a compressible gas volume between the T-junction inlet and a flow control valve. The presence of a compressible gas volume between the T-junction inlet and the flow control valve was found to substantially alter the two-phase flow characteristics in the microchannel, as clearly shown by significantly different void fraction data obtained with and without the compressible gas volume.

The length and velocity of a liquid plug or slug were obtained by cross correlating the signals from two pairs of optical fiber probes placed 1.0 mm apart. The data revealed that short liquid plugs and long liquid slugs can occur in the same microchannel and move with different velocities. The short liquid plugs were found to move with nearly the same velocities as the gas slugs, but long liquid slugs moved at much lower velocities due to friction effects. The liquid slug length data showed both single peak and bimodal distributions, but as the superficial gas velocity was increased, the mean liquid slug length was found to decrease.

ACKNOWLEDGEMENTS

This work was supported by a grant from the Japanese Ministry of Education, Culture, Sports, Science and Technology, and a Discovery research grant from the Natural Sciences and Engineering Research Council of Canada.

NOMENCLATURE

C_1, C_2	Constants in void fraction correlation, Eq. 1
D	Microchannel diameter (m)
j_G	Superficial gas velocity (m/s)
j_L	Superficial liquid velocity (m/s)
L_L	Average length of a liquid plug/slug (m)
u_G	Gas slug velocity (m/s)
U_H	Velocity of a short liquid plug (m/s)
U_i	Velocity of a liquid plug/slug (m/s)
U_L	Velocity of a long liquid slug (m/s)
V/V_o	Output voltage of an optical fiber probe relative to the maximum output voltage
α	Void fraction
β	Homogeneous void fraction
θ	Contact angle

REFERENCES

Ali, M.I., Sadatomi, M., and Kawaji, M., 1993. Two-phase flow in narrow channels between two flat plates. *Can. J. Chem. Eng.*, 71(5), 657-666.

Armand, A.A., 1946. The resistance during the movement of a two-phase system in horizontal pipes. Izv. Vses. Teplotekh. Inst., 1, 16-23 (AERE-Lib/Trans 828).

Cubaud, T., Ulmanella, U., and Ho, C.M., 2004. Two-phase flow in microchannels with surface modifications, Paper No. PL2, Proc. 5th International Conference on Multiphase Flow, ICMF'04, Yokohama, Japan, May 30–June 4, 2004.

Chung, P.M.Y., and Kawaji, M., 2004. The effect of channel diameter on adiabatic two-phase flow characteristics in microchannels. *Int. J. Multiphase Flow*, Vol. 30, No. 7-8, pp. 735-761.

Hughmark, G.A., 1965. Holdup and heat transfer in horizontal slug gas-liquid flow. *Chem. Eng. Sci.*, Vol. 20(12), pp. 1007-1010.

Ide, H., Kimura, R. and Kawaji, M., 2006. Optical Measurement of Void Fraction and Bubble Size Distributions in a Microchannel. Paper ICNMM2006-96100 in *Proc. of 4th International Conference on Nanochannels, Microchannels and Minichannels*, June 19-21, 2006, Limerick, Ireland.

Kawahara, A., Chung, P.M.-Y., and Kawaji, M., 2002. Investigation of two-phase flow pattern, void fraction and pressure drop in a microchannel. *Int. J. Multiphase Flow*, 28(9), pp. 1411-1435.

Kawaji, M., Kawahara, A., Mori, K., Sadatomi, M. and Kumagae, K., 2006. Gas-Liquid Two-phase Flow in Microchannels: the Effects of Gas-Liquid Injection Methods. A Keynote paper in *Proc. of the 7th ISHMT-ASME Heat and Mass Transfer Conference*, 4-6 January 2006, Guwahati, India.

Kawaji, M., Mori, K., and Bolintineanu, D., 2005. The effects of inlet geometry on gas-liquid two-phase flow in microchannels. Keynote Paper No. ICMM2005-75087, *Proc. of ICMM-2005 ASME 3rd International Conference on Microchannels and Minichannels*, June 13-15, 2005, Toronto, Canada.